EPSC Abstracts
Vol. 10, EPSC2015-108, 2015
European Planetary Science Congress 2015

The 9 May 2016 transit of Mercury – a great outreach opportunity in Europe

David A. Rothery (1), Johannes Benkhoff (2) , Joe Zender (2), Ranpal Gill (3), Bernhard Fleck (4), Alain Doressoundiram (5|)
(1) The Open University, Milton Keynes, UK, (2) ESA ESTEC, Noordwijk, Netherlands, (3) ESA ESAC, Madrid, Spain, (4) ESA, c/o NASA/GSFC, Greenbelt, MD, (5) Observatoire de Paris, France (d.a.rothery@open.ac.uk)

Abstract

People across most of the globe will have a chance to witness Mercury's next solar transit, 11:12-18:42 UT, Monday 9 May 2016. Occurring a year after the end of the MESSENGER mission and a few months before the launch of BepiColombo, this transit (the first since 2006) will be an ideal occasion to draw the public's attention to the science goals of those missions, to showcase what we have recently learned about Mercury, and to draw attention to the conundrums that make Mercury such a fascinating object to study.

1. Introduction

Although Mercury passes between the Earth and the Sun at least three times a year, exact alignment is rare and can happen only in May or November, when the Earth is close to one of the two points in its orbit where the two planets' orbital planes intersect. When the alignment is sufficiently exact, Mercury transits across the face of the Sun. Because Mercury's angular size is only about 12" in May (about 1/150th of the Sun's diameter) and 10" in November a magnified image is required to reveal it.

Solar transits of Mercury are more common than those of Venus. The first observation was in 1631 by Pierre Gassendi, thanks to a successful prediction by Johannes Kepler. There is no observational record of a transit of Venus until 1639, even though those can be seen by the naked eye.

Precise observation of planetary transits played a key role in determining the scale of the Solar System, and observing the 3 June 1769 transit of Venus from Tahiti was a primary scientific goal of Captain Cook's first voyage of circumnavigation on HMS Endeavour. Less well known is that the expedition's astronomer Charles Green, along with Cook himself, also observed a transit of Mercury on 9 November 1769, from the shores of Mercury Bay in New Zealand.

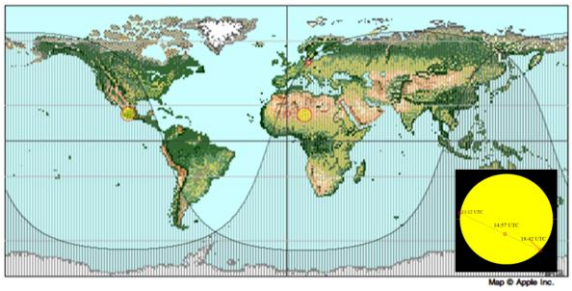

Figure 1: Visibility of Mercury's solar transit, 9 May 2016. The shaded areas limit the hemispheres from which the Sun will be visible at first contact (11:12 UT) and last contact (18:42 UT). Cloud permitting, the whole transit will be visible from most of the Americas and western Europe. Only from a north-south belt from Manchuria to Australia will the whole duration be invisible. (map from http://www.venus-transit.de/Mercury2016/) Inset: the path of Mercury across the Sun, as seen from the northern hemisphere.

2. The 2016 opportunity

The 2004 and 2012 transits of Venus were accompanied by major outreach events, and stimulated day-long media interest. The 2016 Mercury transit offers a similar opportunity, which the Mercury science community should seize upon. It is especially timely for showcasing the science achieved by MESSENGER and planned for BepiColombo. As a bonus, outreach infrastructure and momentum will still be fresh enough to re-use for the next transit, on 11 Nov 2019. Inexpensive

solar projectors adequate to show the transit are readily available, and a recent upsurge of amateurs posting H-alpha and Ca-K solar images via social media shows that the amateur astronomy community is well-equipped to observe the Sun.

2.1 2016 transit outreach plans

Aspirations emerging from the BepiColombo community include:

Encouragement and coordination of schools and local astronomy groups to hold public events during the transit, and to list them on a shared site so that the public can find a nearby event.

Stimulation of national broadcast media to cover the transit, similar to BBC Stargazing's day-long event for the 20 March 2015 solar eclipse and the 2012 and 2004 transits of Venus.

Specific plans include:

Beforehand

Stimulation of awareness and interest via social media, using #MERCURYTRANSIT

Liaison with local and national amateur astronomical societies

Provision of a webportal where groups can advertise events, and that will be searchable by the public

Provision of web-based Mercury and transit outreach materials, to be added to in the months leading up to the transit

Internet advice on safe viewing of the transit

On the day

Webstreaming of images from Proba2, SOHO and SDO spacecraft, and also Hα images every 30 seconds from 9 cm Coronado solar telescopes in Spain and Chile, belonging to the CESAR project (Cooperation through Education in Science and Astronomy Research).

Video–feed, perhaps from ESA-TV, containing pre-recorded features about Mercury and BepiColombo, live or pre-recorded interviews with scientists and engineers

A photo-sharing site where people can post their images of the transit, including a separate area for 'transit selfies'

Experts on Mercury and transits available to talk to the media

What we have already

A humorous animation explaining the relationship between Mercury's day-length and its year http://www.open.edu/openlearn/mercuryday

Transit countdown clock and basic information at http://www.cosmos.esa.int/web/bepicolombo/mercury-transit including a list of public transit events

A facebook 'community' page https://www.facebook.com/mercurytransit2016

3. Summary and Conclusions

We call upon member of the European planetary science and astronomy community to provide transit viewing opportunities for the public in their local area. Please list your event via our website:

http://www.cosmos.esa.int/web/bepicolombo/mercury-transit

EPSC Abstracts
Vol. 10, EPSC2015-184, 2015
European Planetary Science Congress 2015

BepiColombo – a joint ESA/JAXA mission to explore Mercury

J. Benkhoff (1), M. Fujimoto (2) and J. Zender (1)
(1) ESA-ESTEC, SRE-S, Noordwijk, Netherlands (johannes.benkhoff@esa.int , +31 71-5654697), (2) JAXA, 3-1-1 Yoshinodai, 299-8510 Sagamihara, Kanagawa, Japan (fujimoto@stp.isas.jaxa.jp)

Abstract

BepiColombo is a joint project between ESA and the Japanese Aerospace Exploration Agency (JAXA). The Mission consists of two orbiters, the Mercury Planetary Orbiter (MPO) and the Mercury Magnetospheric Orbiter (MMO). The mission scenario foresees a launch of both spacecraft with an ARIANE V in January 2017 and an arrival at Mercury in the first half of 2024. From their dedicated orbits the two spacecraft will be studying the planet and its environment. The MPO scientific payload comprises eleven instruments/instrument packages; the MMO scientific payload consists of five instruments/instrument packages. Together, the scientific payload of both spacecraft will perform measurements to find clues to the origin and evolution of a planet close to its parent star. The MPO on BepiColombo will focus on a global characterization of Mercury through the investigation of its interior, surface, exosphere and magnetosphere. In addition, it will be testing Einstein's theory of general relativity. The MMO provided by JAXA focuses on investigating the wave and particle environment of the planet from an eccentric orbit. Together, the scientific payload of both spacecraft will provide the detailed information necessary to understand the process of planetary formation and evolution in the hottest part of the proto-planetary nebula as well as the similarities and differences between the magnetospheres of Mercury and the Earth.

1. Introduction

A suite of state-of-art scientific instruments allow a wide range of scientific questions to be addressed like understanding of the origin and evolution of a planet close to its parent star, the detailed study of Mercury's figure, its interior structure and composition, the investigation of the interior dynamics and origin of Mercury's magnetic field. Further science goals are trying to understand exo- and endogenic surface modifications, cratering, tectonics, and volcanism. The composition, origin and dynamics of Mercury's exosphere and Mercury's magnetosphere will be addressed by combined measurements of both spacecraft. Last but not least scientist believe that they can use BepiColombo also as a laboratory to test Einstein's theory of general relativity, by performing high accurate positioning measurements of the spacecraft. All in all measurements performed by the instruments on BepiColombo will provide clues on the origin and formation of terrestrial planets and help to answer fundamental questions like: "How do Earth-like planets form and evolve in the Universe?"

Mercury is a small planet compared to the Earth and difficult to observe from the Earth, due to its close proximity to the bright Sun. For an in-depth study ofthe planet and its environment, it is therefore necessary to operate a spacecraft equipped with scientific instrumentation around the planet. On the other hand the thermal and radiation environment close to the Sun and close to the hottest planet in the solar system is extremely aggressive, which makes this mission technically very challenging.

The BepiColombo mission will provide a rare opportunity to collect multi-point measurements in a planetary environment. This will be particularly important at Mercury because of short temporal and spatial scales in the Mercury's environment. It is foreseen that the orbits of MPO and MMO are selected in a way to allow close encounters of the two spacecraft throughout the mission. Such intervals are very important for the inter-calibration of similar instruments on the two spacecraft. They also provide scientifically valuable intervals to collect multi-point measurements in an environment where both spatial and temporal scales can be very short.

In order to ensure the science and technical performance of the spacecraft intense on-ground testing has to be performed. The environment around Mercury imposes strong requirements on the

spacecraft design, particularly to all elements that are exposed to Sun and Mercury.

Recently acceptance testing of the Proto Flight Models (PFM) of the two BepiColombo spacecraft and the Mercury Transfer Module (MTM) are ongoing.

The MTM provides the acceleration and braking required during Cruise to reach the eventual capture by Mercury and the large amount of power required by the solar electric propulsion system. The MTM also constitutes the bottom element in the overall spacecraft structure. The MTM holds 2 solar array wings totaling over 40 m^2, which provide the power for the SEPS (Solar Electric Propulsion System) during the Cruise

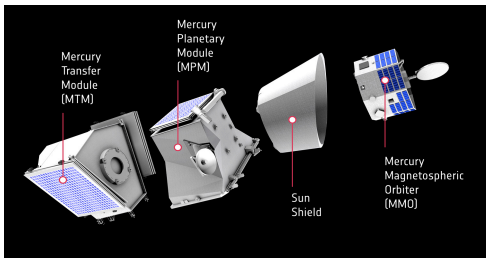

Figure 1: Spacecraft configuration of BepiColombo...

1.1 Science Goals

The main scientific objectives of the BepiColombo mission are to study:

- the origin and evolution of a planet close to its parent star,

- Mercury's figure, interior structure, and composition,

- Interior dynamics and origin of its magnetic field

- Exogenic and endogenic surface modifications, cratering, tectonics, volcanism

- Composition, origin and dynamics of Mercury's exosphere and polar deposits

- Structure and dynamics of Mercury's magnetosphere

- Test of Einstein's theory of general relativity

These questions can be related to five major topical areas, namely interior, surface, exosphere, magnetosphere and fundamental physics.

2. Summary and Conclusions

BepiColombo is the planetary Cornerstone of ESA's Cosmic Vision Programme, and is devoted to the thorough exploration of Mercury and its environment. It will be carried out as a joint project between ESA and the Japanese Aerospace Exploration Agency. The mission consists of two orbiters, the Mercury Planetary Orbiter (MPO), which is 3-axis-stabilised and nadir pointing, and the Mercury Magnetospheric Orbiter (MMO), a spinning spacecraft. With its two-spacecraft, interdisciplinary approach, the BepiColombo mission will provide the detailed information necessary to understand the processes of planetary formation and evolution in the hottest part of the proto-planetary nebula, as well as the similarities and differences between the magnetospheres of Mercury and Earth. To accomplish this, a global characterisation of Mercury is required, which will be achieved with a thorough investigation of its interior, surface, exosphere and magnetosphere. In addition, the mission offers unique possibilities for testing Einstein's theory of general relativity.

The BepiColombo mission to Mercury has a large scientific interest in Europe and Japan and will expand our knowledge of planetary formation in close proximity to its parent star. BepiColombo will provide comprehensive, high-resolution global coverage of the planet, infrared images, surface composition, and global temperature maps. It aims for a global 3-dimensional (stereo) coverage of the surface, accurate measurements of Mercury's gravity field (planet interior, test of Einstein's theory) and high-detailed measurements of the plasma and particle environment
Last but not least BepiColombo will follow up on MESSENGER results and will to close the gaps in the southern hemisphere

References

[1] Benkhoff, J., van Casteren, J., Hayakawa, H., Fujimoto, M., Laakso, H., Novara, M., Ferri, P., Middleton, H. R., and Ziethe, R. BepiColombo—Comprehensive exploration of Mercury: Mission overview and science goals Planetary and Space Science, Volume 58, Issue 1-2, p. 2-20, 2010.

EPSC Abstracts
Vol. 10, EPSC2015-259, 2015
European Planetary Science Congress 2015

A quasi-hemispheric model of the Hermean's magnetic field

E. Thébault , J. Oliveira, B. Langlais and H. Amit
University of Nantes, LPGNantes, CNRS - UMR 6112, Nantes, France (erwan.thebault@univ-nantes.fr)

Abstract

We analyse and process magnetic field measurements provided by the MErcury Surface, Space ENvironment, Geochemistry, and Ranging (MESSENGER) mission. The vector magnetic field measurements are modelled with a dedicated regional scheme expanded in space and in time. Compared to the widely used global Spherical Harmonics (SH), the regional approach is particularly well suited because the partial and quasi hemispheric distribution of the MESSENGER data represents no major numerical difficulty. We confirm that the internal magnetic field of Mercury is mostly axisymmetric with a magnetic equator shifted northward. However, we also observe a time dependency in the model that is at present hardly explained only by time variations of the external magnetic fields. We present the major spatial and temporal structures shown by the regional model.

1. Introduction

One of the objectives of the MESSENGER spacecraft was to better describe the magnetic fields surrounding the planet Mercury and to better understand their origin. The magnetic measurements are acquired by MESSENGER along a near polar but very elliptical orbit and are useful for internal magnetic field studies mostly above the northern hemisphere. This orbital configuration challenges our ability to separate the measured magnetic fields into their internal and external contributions and to model them globally to high spatial resolution using classical mathematical techniques such as the spherical harmonics ([1], [2]).
In the recent years, attempts have been made to circumvent this difficulty using dedicated regional or local techniques. Such techniques could rely on an equivalent representation of sources (e.g. [3]) using hypotheses about the location of the magnetic field sources. However, other techniques inherited from Earth's studies based on regional mathematical functions could equally be applied without the need for a priori information about the sources. In this paper, we apply the Revised Spherical Cap Harmonic Analysis ([4]) to derive a magnetic field model from the magnetic field measurements of the MESSENGER spacecraft. Then, we analyse the distribution of the residuals in space and in time. From this analysis, we update the model and incorporate time varying functions to represent the data in space and in time. We finally attempt to separate accurately internal and external fields.

2. Model and Results

We consider three terrestrial years of MESSENGER measurements from March 2011 to April 2014. Measurements recorded after April 2014 cover a too small portion of the Northern hemisphere and are thus discarded. We keep all measurements near the periapsis (down to about 200 km altitude) but reject all measurements taken above 1100 km altitude to reduce the influence of magnetospheric field currents in the data. The measurements cover all local times and colatitudes from 0 to about 85° and are thus available over most of the Northern hemisphere (excluding the polar data gap). We assume that the selected data are measured in source free region and apply the R-SCHA potential field modeling technique to fit the measurements in space. We derive the preliminary model to a horizontal spatial wavelength equal to about 800 km (corresponding to a maximum truncation degree equal to 20 in spherical harmonics). The data misfit is about 30 nT for the static part and the correlation between the vector data and the model is better than 0.97.
The model in space is mostly axisymmetric and the magnetic equator is found around latitude 10°N. From the regional spatial power spectrum we estimate that the CMB is located at about 350-400 km depth below the mean Mercury's radius. The computation of the azimuthal power spectrum (in function of the orders m) shows that the static model is explained at 99% by zonal terms. These results are in agreement with previous studies ([1], [2] and [3]). We then analyze the distribution of the residuals in space and in time. The residuals show clear structures in space and in time. We see a sharp increase in the misfit scatter with the altitude around 300 km that is not linked to a well-defined physical process. The time variations of the residuals are also closely related to the position of the Sun. However, we show that these features cannot be easily explained in terms of external magnetic field only. We then iterate the regional model including time dependencies. This reduces the final data misfit to about 13 nT and increases the correlation between the data and the model up to 0.99.

Acknowledgements

This work is partly funded through the ANR project MARMITE (ANR-13-BS05-0012) and PNP/INSU/CNRS program.

References

[1] Anderson, B. J., Johnson, C. L., Korth, H., Winslow, R. M., Borovsky, J. E., Purucker, M. E., ... & McNutt, R. L. (2012). Low-degree structure in Mercury's planetary magnetic field. Journal of Geophysical Research: Planets (1991–2012), 117(E12).

[2] Johnson, C. L., Purucker, M. E., Korth, H., Anderson, B. J., Winslow, R. M., Al Asad, M. M., ... & Solomon, S. C. (2012). MESSENGER observations of Mercury's magnetic field structure. Journal of Geophysical Research: Planets (1991–2012), 117(E12).
[3] Oliveira, J. S., Langlais, B., Pais, M. A., and Amit, H.: A modified method to model partially distributed magnetic field measurements, with application to Mercury. Journal of Geophysical Research (Planets), under review.
[4] Thébault, E., Schott, J. J., & Mandea, M. (2006). Revised spherical cap harmonic analysis (R-SCHA): Validation and properties. Journal of Geophysical Research: Solid Earth (1978–2012), 111(B1).

EPSC Abstracts
Vol. 10, EPSC2015-455, 2015
European Planetary Science Congress 2015

SYNTHETIC GLASSES AS ANALOGS FOR INFRARED STUDIES OF PLANETARY SURFACES

A. Morlok (1), S. Klemme (2), I. Dittmar (3), A. Stojic (1), I.Weber (1), H.Hiesinger (1), M.Sohn (3), J.Helbert (4)
(1) Institut für Planetologie, Wilhelm-Klemm Strasse 10, 48149, Germany (morlokan@uni-muenster.de)
(2) Institut für Mineralogie, Corrensstraße 24, 48149 Münster, Germany (3) Hochschule Emden/Leer, Constantiaplatz 4, 26723 Emden, Germany (4) Institute for Planetary Research, DLR, Rutherfordstrasse 2, 12489 Berlin, Germany.

Abstract

We present mid-infrared spectra of glasses with the chemical composition of surface areas from Mercury based on MESSENGER data. The data will be used for the interpretation of results of the MERTIS mid-infrared spectrometer on the ESA/JAXA BepiColombo mission to Mercury.

1. Introduction

Our work at the IRIS (InfraRed spectroscopy for Interplanetary Studies) laboratory produces spectra for a database for the ESA/JAXA BepiColombo mission to Mercury. Onboard is a mid-infrared spectrometer (MERTIS-Mercury Radiometer and Thermal Infrared Spectrometer). This unique device allows us to map spectral features in the 7-14 µm range, with a spatial resolution of ~500 m [1-4]. These infrared spectra allow determining the mineralogical compositions of the planetary surface via remote sensing. Material on the surface of Mercury was exposed to heavy impact cratering in its history [4]. Glass lacks an ordered microstructure and represents the most amorphous phase of a material, typical for events generated by events involving high shock pressure and temperatures [5,6]. Using synthetic materials allows us to produce infrared spectra of analogue materials based on the observed chemical composition of planetary bodies, from which no material in form of meteorites is available.

Here we present glasses with the composition of the large surface regions G1 and G2 on Mercury, based on MESSENGER data [7]. G1 is an area in the equatorial region of Mercury, and area G2 is on the southern hemisphere.

2. Samples and Techniques

Preparation of Glass: We prepared starting material mixtures of oxides (SiO_2, TiO_2, Al_2O_3, Fe_2O_3, MgO and carbonates ($CaCO_3$) with the composition of the large surface regions G1 and G2. The finely ground powder was slowly heated to 1000°C to decarbonate and subsequently vitrified in a vertical furnace at 1500°C for 2 h and quenched immediately afterwards.

Characterization: The resulting glass was embedded in resin and polished to a thin section. The amorphous character was confirmed by optical petrological microscopy. The chemical composition of the glass was analyzed using a JEOL 6610-LV Scanning electron microscope equipped with an Oxford silicon drift electron dispersive EDX system. A fully standardized quantitative analysis was performed using ASTIMEX™ mineral standards.

FTIR Analyses: For in-situ mid-infrared specular reflectance analyses we used a Bruker Hyperion 2000 System at the Hochschule Emden/Leer. We used a 1000*1000 (μm^2) sized aperture, for each spectrum; 128 scans were added. A Bruker Vertex 70 infrared system with a MCT detector at the Institut für Planetologie was applied for analyses of powdered material in near vacuum. To ensure high signal to noise ratio, we accumulated 512 scans for each size fraction. For background calibration, we used a well calibrated gold standard.

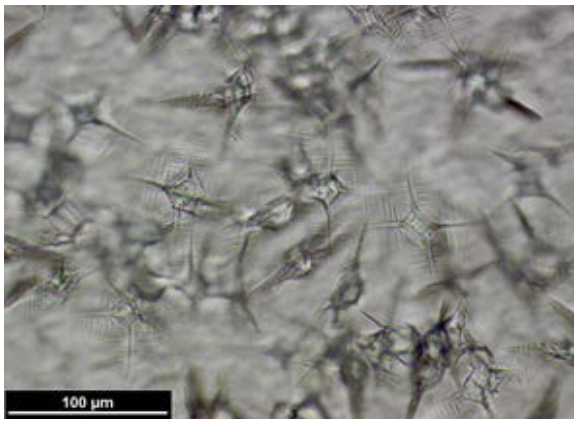

Figure 1: Optical microscope image of small crystallites in the glass, forming a spinifex texture.

3. Results

Optical polarization microscopy shows a glass with abundant small crystalline inclusions showing spinifex textures in glass G1 (Fig.1).

The spectra of grain size fractions for surface areas G1 and G2 on Mercury (Fig.2a, b) show Christiansen Features (CF) at 8.0-8.2µm, and a strong amorphous silicate Reststrahlen-Band (RB) at 10.3-10.5 µm. Area G1 also shows some weak crystalline features of forsterite [8] at 10.1 and 10.4 µm. Transparency Features (TF) are weak and occur at 11.8-12.2 µm.

Spectra obtained for G1 and G2 using micro-FTIR of inclusion-free spots confirm the findings.

4. Summary and Conclusions

Both glasses show a very high degree of crystallinity, even the abundant small spinifex crystals in G1 only create very weak bands in the mid-infrared.

In our presentation, we will show glasses with the compositions of many more surface areas of Mercury, as well as of models for the bulk mantle compositions of the planet.

References

[1] Maturilli A. (2006) Planetary and Space Science 54, 1057–1064.

[2] Helbert J. and Maturilli A. (2009) Earth and Planetary Science Letters 285, 347-354.

[3] Benkhoff, J. et al. (2010) Planetary and Space Science 58, 2-20.

[4] Hiesinger H. et al. (2010) Planetary and Space Science 58, 144–165.

[5] Johnson (2012) Icarus 221, 359–364

[6] Lee et al. (2010) Journal of Geophysical Research 115, 1-9

[7] Charlier B. et al. (2013) Earth and Planetary Sci-ence Letters 363, 50–60.

[8] Hamilton V. E. (2010) Chemie der Erde 70, 7-33.

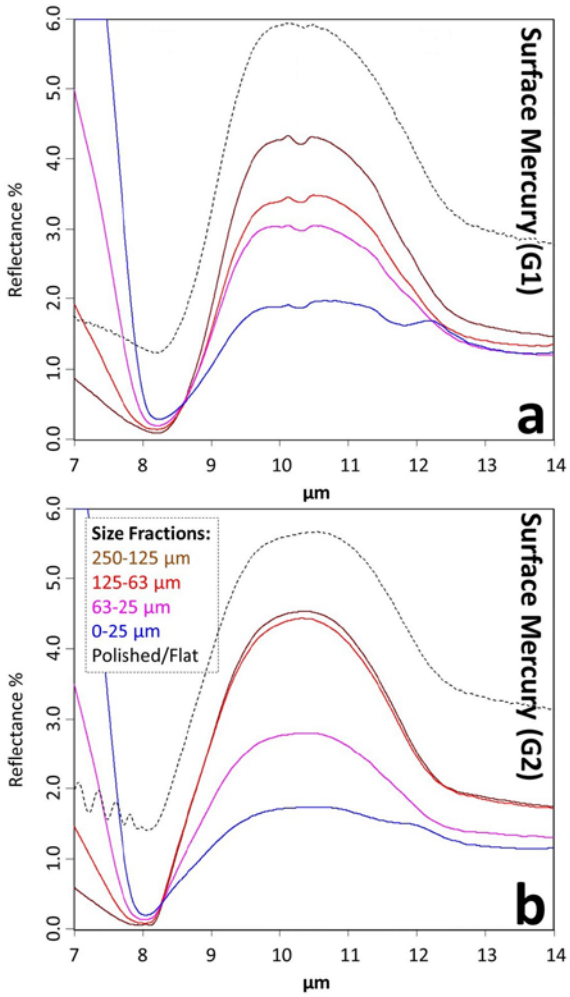

Figure 2: Mid-IR reflectance spectra of two bulk size fractions of synthetic glasses and in-situ analyses of thin sections in the range of the BepiColombo MERTIS spectrometer (in microns; µm).

Acknowledgements

This work is supported by the DLR funding 50 QW 0901 in the framework of the BepiColombo mission.

EPSC Abstracts
Vol. 10, EPSC2015-485, 2015
European Planetary Science Congress 2015

Equilibrium Obliquity of Mercury: Effect of the inner core and the pericenter

M. Yseboodt[1], R.-M. Baland[2 1], T. Van Hoolst[1], A. Rivoldini[1]
[1] Royal Observatory of Belgium, Brussels, Belgium (m.yseboodt@oma.be),
[2] Université catholique de Louvain, Earth and Life Institute, Louvain-la-Neuve, Belgium

1. The Cassini state

Mercury's spin axis has been shown to occupy the Cassini state 1 (Margot et al. 2007, 2012). In this equilibrium state, the orbit normal, the spin axis and the normal to the Laplace plane remain coplanar, precessing all together with a very long period of about 300 000 years. The obliquity stays constant with time.

Up to now, the Cassini state and the corresponding equilibrium obliquity have only been investigated for a planet with a solid layer and a fluid core. In this study, we investigate the effect of an ellipsoidal inner core and the precession of the pericenter on the equilibrium obliquity.

2. Ellipsoidal Inner Core

We consider a planet with 3 layers: a solid mantle (including the crust), a fluid outer core and a solid inner core. The interior models are constrained by the mass, the radius, the gravity field coefficients and the observed libration amplitude. Different assumptions are used to compute the equatorial and polar flattening of each layer (see Yseboodt et al. 2013).

Using a method similar to Baland et al. (2012), we investigate the effect of a non spherical inner core on the equilibrium obliquity. Since the orbital plane is precessing about the Laplace plane, we express the motion of the spin axis in a frame based on the Laplace plane.

We take into account the following torques on each layer: the solar gravitational torque on the layers, the pressure torque on the mantle and the inner core, and the gravitational torque between the mantle and the inner core. We also add dissipative viscous torques.

3. Precession of the pericenter

The longitude of the pericenter ω of Mercury around the Sun has a slow precessional motion of about 127 000 years. In order to compute the motion of the spin axis, the solar gravitational torque has to be averaged over the fast motions like the anomaly of Mercury. The pericenter precession is not a fast angle, therefore we keep the terms depending on the argument of the pericenter and evaluate the effect of this motion on the equilibrium obliquity.

References

- Baland R.-M. et al., Obliquity of the Galilean satellites: The influence of a global internal liquid layer, Icarus 220, 2012.
- Margot J.L. et al., Large longitude libration of Mercury reveals a molten core, Science 316, 2007.
- Margot J.L. et al., Mercury's moment of inertia from spin and gravity data, J. Geophys. Res., 2012.
- Peale et al., Effect of core-mantle and tidal torques on Mercury's spin axis orientation, Icarus 231, 2014.
- Yseboodt M. et al., Influence of an inner core on the long-period forced librations of Mercury, Icarus 226, 2013.

Acknowledgment

R.M.B. is funded by a FSR (Fonds Spécial de Recherches) grant from UCL. This work was financially supported by the Belgian PRODEX program managed by the European Space Agency in collaboration with the Belgian Federal Science Policy Office.

EPSC Abstracts
Vol. 10, EPSC2015-517, 2015
European Planetary Science Congress 2015

The origin of the compositional diversity of Mercury's surface constrained from experimental melting of enstatite chondrites

A. Boujibar (1), K. Righter (1), K. Pando (2) and L. Danielson (3).
(1) NASA Johnson Space Center, Houston, USA, [2]UTAS – Jacobs JETS Contract, NASA Johnson Space Center, Houston, USA, [3]Jacobs JETS, NASA Johnson Space Center, Houston, USA. (asmaa.boujibar@nasa.gov).

1. Introduction

Mercury is known as an endmember planet as it is the most reduced terrestrial planet with the highest core/mantle ratio. MESSENGER spacecraft has shown that its surface is FeO-poor (2-4 wt%) and S-rich (up to 6-7 wt%) [1-2], which confirms the reducing nature of its silicate mantle [3]. Moreover, high resolution images revealed large volcanic plains and abundant pyroclastic deposits [4], suggesting important melting stages of the Mercurian mantle. This interpretation was confirmed by the high crustal thickness (up to 100 km) derived from Mercury's gravity field [5]. This is also corroborated by a recent experimental result that showed that Mercurian partial melts are expected to be highly buoyant within the Mercurian mantle and could have risen from depths as high as the core-mantle boundary [6].

In addition MESSENGER spacecraft provided relatively precise data on major elemental compositions of Mercury's surface [7]. These results revealed important chemical and mineralogical heterogeneities that suggested several stages of differentiation and re-melting processes [8]. However, the extent and nature of compositional variations produced by partial melting remains poorly constrained for the particular compositions of Mercury (very reducing conditions, low FeO-contents and high sulfur-contents). Therefore, in this study, we investigated the processes that lead to the various compositions of Mercury's surface. Melting experiments with bulk Mercury-analogue compositions were performed and compared to the compositions measured by MESSENGER.

2. Methods

Experiments were conducted with a piston cylinder apparatus at NASA JSC at 1 GPa and temperatures between 1400°C and 1650°C, using enstatite chondrites (EH4), with variable oxygen fugacity and sulfur content. By varying the Si/SiO_2 ratio of the starting composition, we could control the fO_2 of the experiments. We used two starting compositions with two different sulfur contents, Si/SiO_2 ratios and oxygen fugacity (see **Table 1**). Experimental run products were analyzed with Cameca and JEOL EPMAs at NASA JSC.

3. Results

3.1 Oxygen fugacity

The oxygen fugacity of the samples was calculated relative to the IW buffer and Si/SiO_2 buffer. The fO_2 was estimated at IW-3 and IW-6 for the composition 1 and composition 2 respectively (see **Table 1**).

3.2 Phase proportions

The samples synthesized with the compositions 1 and 2 are both composed of orthopyroxene, silicate melt and liquid metal at high temperature. For composition 1, when T<1450°C, quartz is also present in the samples, while for composition 2, at T<1500°C, a liquid sulfide is also present. However this sulfide phase represents only 1 to 3% of the experimental charges. This is due to sulfur volatilization during the heating of the samples. Indeed mass balance calculations show that at least half the initial content of sulfur was volatilized during sample heating. In addition the samples synthesized with the most S-rich composition are also very reduced, so that S is highly solubilized in the silicate melt (with S-concentrations up to 9 wt%).

3.3 Evolution of the silicate melts compositions

Our data are combined with previous experiments performed at 1 bar [9] with EH4 enstatite chondrite [10] as starting composition which is closer to our

synthetic composition 2. Incompatible elements (Na, K, Al, Si) decrease with temperature while compatible elements (Mg) increase with temperature. Major differences between the experiments conducted with the starting composition 1 and 2 are the enrichment in SiO_2 in the silicate melts with the first composition in comparison to the second one. At 1 bar the presence of large fractions of Ca-rich sulfide significantly affects the behavior of CaO in the silicate melt. At 1 GPa, sulfide is only present in low proportions (<3 wt%), therefore it does not have any effect on the CaO concentration of the silicate melt.

4. Comparison with Mercury's surface:

Ca/Si, Mg/Si and Al/Si element ratios of our silicate melts and that of previous studies [9] are compared to that of Mercury's surface in **Fig. 1**. We found that the melts produced with composition 1 have lower Al/Si and Ca/Si ratios than Mercury's surface. This can be due to the high SiO_2 of the starting composition 1. On the other hand, the compositions of Mercury's surface are in a good match with the silicate melts synthesized with the S-rich starting material (this study, composition 2) and the samples run at 1 bar by [9] with EH4 chondrites.

Our results show that melting at various pressures of sulfur-rich EH4 chondrites can generate liquids with a high diversity in chemical composition. The heterogeneous compositions observed on the surface of Mercury can be explained by the melting of a chondritic mantle at different depths extending at least to 55 km and relatively high temperatures comprised between 1300 and 1550 °C with 10 to 45 weight % of melting. Hence, it is not required to invoke several stages of differentiation and re-melting processes to explain the Mercurian surficial compositions derived from MESSENGER results [2, 6]. Additional experimental work is underway and will provide better constraints on the effects of sulphur and pressure on the physical and chemical properties of the Mercurian mantle.

4. Tables

Table 1: Starting compositions used in our experiments. The concentrations of all other elements than S and Si are similar than in EH4 enstatite chondrites [10].

Composition 1	Composition 2
62/38 silicate/metal	50/50 silicate/metal
5 wt% Si in metal	12 wt% Si in metal
59 wt% SiO_2 in silicate	50 wt% SiO_2 in silicate
2 wt% bulk S	6 wt% bulk S

6. Figures

Figure 1: Comparison between Al/Si, Mg/Si and Ca/Si ratios of Mercury's surface (asterix) [7,11] with the melting products of enstatite chondrites (1 GPa this study, blue circles and yellow squares and 1 bar from [9], green triangles).

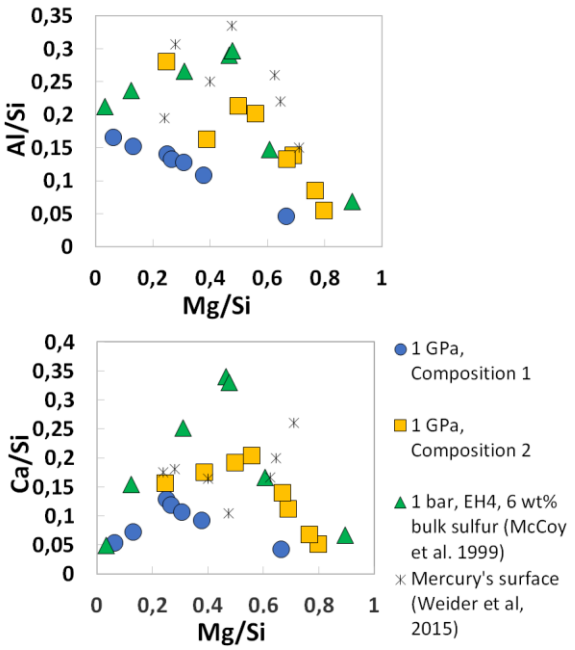

References

[1] McClintock W. E. et al., Science, Vol. 321, pp. 62-65, 2008. [2] Nittler L. R. et al., Science, Vol. 333, pp. 847-1850, 2011. [3] Zolotov M. Y. et al., JGR, Vol. 118, pp. 138-146, 2013. [4] Head J. W. et al., Science, Vol. 333, pp. 1853-1856, 2011. [5] Smith D. E. et al., Science, Vol. 336, pp. 214-217, 2012. [6] Vander-Kaaden K. E. and McCubbin F., JGR, Vol. 120, pp. 195-209, 2015. [7] Weider S. Z. et al., EPSL, Vol. 416, pp. 109-120, 2015. [8] Charlier B. et al., EPSL, Vol. 363, pp. 50-60, 2013. [9] McCoy T. J. et al., Meteoritics & Planet. Sci., Vol. 34, pp. 735-746, 1999. [10] Wiik H. B., GCA, Vol. 9, pp. 279-289, 1956. [11] Namur O. et al., LPSC abstract 1309, 16-20 May 2015, The Woodlands, USA.

EPSC Abstracts
Vol. 10, EPSC2015-570, 2015
European Planetary Science Congress 2015

Mercury's thermal evolution and core crystallization regime

A. Rivoldini(1), T. Van Hoolst(1), M. Dumberry(2) and G. Steinle-Neumann(3)
(1) Observatoire Royal de Belgique, Belgium (attilio.rivoldini@oma.be), (2) Department of Physics, University of Alberta, Canada, (3) Bayerisches Geoinstitut, University of Bayreuth, Germany

Abstract

Unlike the Earth, where the liquid core isentrope is shallower than the core liquidus, at the lower pressures inside Mercury's core the isentrope can be steeper than the melting temperature. As a consequence, upon cooling, the isentrope may first enter a solid stability field near the core mantle boundary and produce iron-rich snow that sinks under gravity and produces buoyant upwellings of iron depleted fluid. Similar to bottom up crystallization, crystallization initiated near the top might generate sufficient buoyancy flux to drive magnetic field generation by compositional convection.

In this study we model Mercury's thermal evolution by taking into account the formation of iron-rich snow to assess when the conditions for an internally magnetic field can be satisfied. We employ a thermodynamic consistent description of the iron high-pressure phase diagram and thermoelastic properties of iron alloys as well as the most recent data about the thermal conductivity of core materials.

We use a 1-dimensional parametrized thermal evolution model in the stagnant lid regime for the mantle (e.g. [1]) that is coupled to the core. The model for the mantle takes into account the formation of the crust due to melting at depth. Mantle convection is driven by heat producing radioactive elements, heat loss from secular cooling and from the heat supplied by the core.

The heat generated inside the core is mainly provided from secular cooling, from the latent heat released at iron freezing, and from gravitational energy resulting form the release of light elements at the inner core-outer core boundary as well as from the sinking of iron-rich snow and subsequent upwellings of light elements in the snow zone. If the heat flow out of the core is smaller than the heat transported along the core isentrope a thermal boundary will from at the top of the outer core. To determine the extension of the convecting region inside the liquid core we calculate the convective power [2]. Finally, we use the entropy budget of the core (e.g. [3]) together with the core mantle boundary heat flow to assess whether a magnetic field can be generated and sustained inside Mercury's core.

Acknowledgements

This work was financially supported by the Belgian PRODEX program managed by the European Space Agency in collaboration with the Belgian Federal Science Policy Office

References

[1] A. Morschhauser, M. Grott, and D. Breuer, "Crustal recycling, mantle dehydration, and the thermal evolution of Mars," *Icarus*, vol. 212, no. 2, pp. 541 – 558, 2011.

[2] H. Gomi, K. Ohta, K. Hirose, S. Labrosse, R. Caracas, M. J. Verstraete, and J. W. Hernlund, "The high conductivity of iron and thermal evolution of the Earth's core," *Physics of the Earth and Planetary Interiors*, vol. 224, pp. 88–103, 11 2013.

[3] F. Nimmo, "Thermal and Chemical Evolution of the Core," in *Evolution of the Earth* (D. J. Stevenson, ed.), vol. 9 of *Treatise in Geophysics*, Elsevier, Amsterdam, 2007.

EPSC Abstracts
Vol. 10, EPSC2015-630, 2015
European Planetary Science Congress 2015

Calibration activities on the BepiColombo High-Resolution Channel (HRIC) of SIMBIO-SYS instrument

V. Della Corte(1), M. Zusi(1,2), M. Baroni(3), I. Ficai Veltroni(3), P. Palumbo(4), E. Flamini(5), R. Mugnuolo(6)
(1) INAF-IAPS, Roma, IT, (2) INAF-OAC, Napoli, IT , (3) SelexES, Campi Bisenzio (FI), IT , (4) DiST, Universit Parthenope, Napoli, IT, (5) ASI, Roma, IT, (6) ASI, Matera, IT.

Abstract

HRIC (High Resolution Imaging Channel) is the high resolution channel of the SIMBIO-SYS instrument onboard the ESA BepiColombo Mission. Calibration activities were performed at SelexES premises in spring-summer 2014 in order to check for Channel performances (radiometric performances, quality image and geometrical performances) and to obtain data necessary to setup a calibration pipeline necessary to process the raw images acquired by the channel when in operative scenario.

1. Introduction

Main measured parameters include electrical parameters of the channel (readout noise, fixed pattern noise, dark current); radiometric performances (response vs. integration time and flux spectral response). All parameters have been measured at pixel level due to the relatively high variability of CMOS detectors with respect to CCDs. The final target is to obtain parameters for the calibration pipeline correcting pixel-by-pixel HRIC data.

2. Calibration Setup Performed Measurements

The test has been performed in cleanroom class 100,000 where the HRIC OGSE and TVC have been placed for the entire HRIC PFM test campaign. The test set-up employed for the performed Performance Tests is shown in Figure 1 and mainly is composed of the TVC where the flight hardware is mounted, the TVC control system, the UT to control HRIC during the operative phases of the test and the OGSE to provide the optical stimulus through the optical window of the TVC (Fig.1). By means of the the collected data we characterized :

- The Dark Current (DC) behaviour
- The Read Out Noise (RON) of the detector
- The Fixed Pattern Noise (FPN)
- The Photo Response and the Photo Response Non Uniformity (PRNU)
- the Radiometric performances

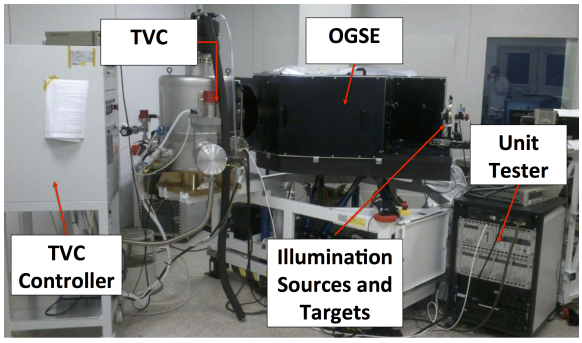

Figure 1: Experimental Setup used during the HRIC calibration campaign.

3. Results

3.1 Dark Current

The DC shows a double trend, in fact while for very short integration times (t_{exp} < 0,05 ms) the DC shows a high rate that can be fitted as a quadratic function of the exposure time, for t_{exp}> 0.05 ms the DC shows a smooth and relatively small linear rate well within the requirements. The DC behavior has an impact on data calibration only for very short integration times, for exposure greater than 0.05 ms.

3.2 Read Out Noise and Fixed Pattern Noise

Due to the behaviour shown by the dark current, we evaluated the RON and the FPN at two different value

of integration time: for $t_{exp} << 0.05$ ms and for $t_{exp} > 0.05$ms (Fig. 2). This approach simplifies the evaluation of the right parameters that have to be applied to the raw images in order to have calibrated data.

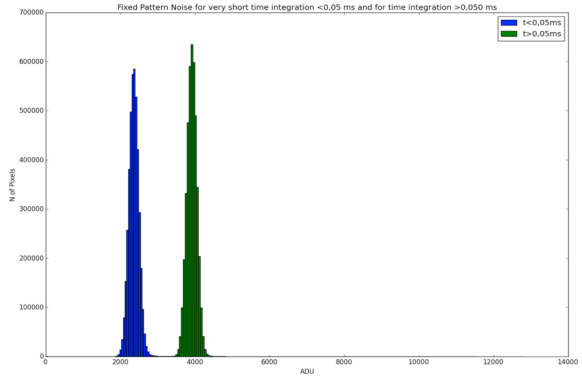

Figure 2: Different distribution for FPN considering the different behavior for very small integration time

3.3 Linearity

The response of each pixel of the channel vs. integration time and vs. light flux intensity has been characterized. The high resolution channel has a response with respect to the flux very close to linearity considering about 80% of the available signal range. Moreover the characterization of the response of each pixel allows us to remove the PRNU from the images (Fig. 3).

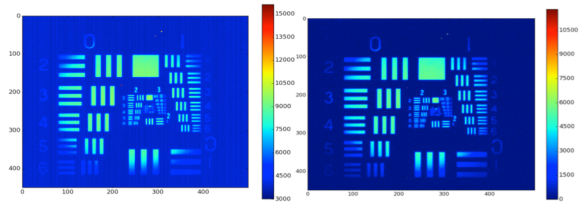

Figure 3: Left Panel raw acquired image; Right Panel Image after DC, FPN and PRNU removal.

4. Summary and Conclusions

Thanks to the characterization of the HRIC Channel obtained during the calibration campaign a first test of low level image processing has been performed. The on-going analysis activity on the acquired data is devoted to fully characterize the radiometric and geometrical performances of SIMBIO-SYS high resolution channel.

Acknowledgements

This research was supported by the Italian Space Agency (ASI) within the SIMBIOSYS project (ASI-INAF agreement n. I/022/10/0).

EPSC Abstracts
Vol. 10, EPSC2015-657, 2015
European Planetary Science Congress 2015

Hermean magnetic field models based on MESSENGER measurements

J. S. Oliveira (1,2), B. Langlais (1), M. A. Pais (2), and H. Amit (1)
(1) Laboratoire de Planétologie et Géodynamique, LPGNantes, CNRS UMR6112, Université de Nantes, Nantes, France
(2) CITEUC, Departament of Physics, University of Coimbra, Portugal (joana.oliveira@univ-nantes.fr)

Abstract

We model the magnetic field of Mercury as measured by the MESSENGER spacecraft during the first six Hermean years using a modified method based on the Equivalent Source Dipole (ESD) approach [1]. We analyze models using different data sets. First we analyze models using eighteen sidereal days separately. Because a periodic signal is observed each 3 sidereal days, we also analyze models of each solar day, corresponding to three consecutive sidereal days. Finally we analyze a model that contains all eighteen sidereal-day measurements together, termed the 6-solar-day model. At the timescale of 1 and 6 solar days, no coherent non-axisymmetric feature is recovered by our method, which was designed to recover an arbitrary internal field. We conclude that this provides strong evidence for the large-scale and close-to-axisymmetry structure of the internal magnetic field of Mercury.

1. Introduction

The internal magnetic field of Mercury is much weaker than that expected from a magnetostrophic force balance. Explaining this feature as well as unraveling the field morphology are among the objectives of the MESSENGER spacecraft which has been in orbit around Mercury since 2011. MESSENGER flies on a very eccentric, near-polar orbit, with a periapsis at 200 km altitude in the northern hemisphere. Because of the weak internal magnetic field, MESSENGER is inside the Hermean magnetosphere only during a short portion of its orbit, and data with a high internal to external field ratio are available only above the northern hemisphere. Global methods such as the spherical harmonics are therefore not directly applicable without using regularizations that would introduce some arbitrariness. We apply a modified ESD method in order to model the Hermean magnetic field above the northern hemisphere.

The ESD method was developed to reduce to a common altitude static fields of lithospheric origin, induced by magnetized sources at shallow depths [2]. It has been adapted to the case of remanent magnetic fields on Mars, where all three components of the measured magnetic field are used to constrain the three components of the magnetization [3, 4].

2. Method

We apply the ESD method with a deeper localization of the sources (inside the core of Mercury), in order to model and describe Mercury's core magnetic field at the altitude of MESSENGER [1]. This new approach has been validated for measurements predicted on regular grids and along MESSENGER orbits, with a synthetic geomagnetic field model scaled to the geometry and intensity of Mercury. In both cases the field is successfully recovered at measurement altitude. We also tested the altitude range to upward or downward continue the modeled magnetic field. For synthetic measurements along MESSENGER orbits this altitude range is 10 to 970 km with an error lower than 8% with respect to the initial scaled model.

3. MESSENGER data and models

Our method is applied to the first eighteen Hermean sidereal days separately, where each sidereal day corresponds to a complete longitudinal coverage of the northern hemisphere. Modeled magnetic field maps at body-fixed coordinates are obtained at 200 km altitude for each sidereal day, as well the corresponding residual maps. In these models and residual maps we find small scale features rotating around the planetary rotation axis from one sidereal day to the other, and repeating each 3 sidereal days. This observation together with the 3:2 spin-orbit resonance suggest that these small-scale rotating features have an external origin.

We then model complete solar days (three consecutive sidereal days) separately and obtain solar-day

models. Those solar-day maps show reduced small-scales compared to the sidereal-day models, with a ratio of non-zonal radial field rms to total radial field rms lower than 12%, revealing that the field is dominantly axisymmetric.

Finally, we apply our method to all eighteen sidereal days together (or all 6 solar days). This 6-solar-day model, which is our most robust model, shows a dominantly axial dipolar field and contains a ratio of non-zonal radial field rms to total radial field rms comparable to the previous solar-day models. Converting this model into a spherical harmonic expansion, we obtain a stronger quadrupole-to-dipole ratio of 0.48 ± 0.03 and a weaker octupole-to-dipole ratio of 0.07 ± 0.01 compared to those obtained by [5]. A very small tilt of 0.92° is also obtained from the converted 6-solar-day model, slightly larger than the upper bound found by [5].

4. Discussion and Conclusions

We apply a modified ESD method to the global magnetic field of Mercury. When applying our method to MESSENGER data for each sidereal day, small scale features of the modeled magnetic field are rotating around the planetary rotation axis between each sidereal day, repeating each 3 sidereal days. These small scale features diminish when we model complete solar days of Mercury, suggesting that these features likely result from external sources. Temporal variations from one consecutive solar day to another are axisymmetric and vary substantially with time, but the rms difference remains lower than 80 nT. This suggests that some large-scale external fields are modeled together with the internal magnetic field. Our results call for a future development of a method to jointly model the internal and external fields. However, we emphasize that the lack of any coherent non-axisymmetric feature recovered by our method provides strong evidence for the large-scale and close-to-axisymmetry structure of the internal magnetic field of Mercury.

Acknowledgements

This work is partly funded through the ANR project MARMITE (ANR-13-BS05-0012) and PNP/INSU/CNRS program.

References

[1] Oliveira, J. S., Langlais, B., Pais, M. A., and Amit, H.: A modified method to model partially distributed magnetic field measurements, with application to Mercury. Journal of Geophysical Research (Planets), manuscript in revision.

[2] Mayhew, M. A.: Inversion of satellite magnetic anomaly data. Journal of Geophysics, 1979.

[3] Purucker, M., Ravat, D., Frey, H., Voorhies, C., Sabaka, T., and Acuña, M.: An altitude-normalized magnetic map of Mars and its interpretation. Geophysics Research Letters, 2000.

[4] Langlais, B., Purucker, M. E., and Mandea, M.: Crustal magnetic field of Mars. Journal of Geophysical Research (Planets), 2004.

[5] Anderson, B. J., Johnson, C. L., Korth, H., Winslow, R. M., Borovsky, J. E., Purucker, M. E., Slavin, J. A., Solomon, S. C., Zuber, M. T., and McNutt, Jr., R. L.: Low-degree structure in Mercury's planetary magnetic field. Journal of Geophysical Research (Planets), 2012.

EPSC Abstracts
Vol. 10, EPSC2015-797, 2015
European Planetary Science Congress 2015

The Missing Mantle Paradox, and the Statistical Argument for Repeated Hit and Run Collisions

E. Asphaug (1) and A. Reufer (1)
(1) Arizona State University, Tempe AZ, email: easphaug@asu.edu

Abstract

Mercury's formation can be explained by a giant impact. However, a direct hit blasting off the mantle [1] leaves debris stranded in orbit about the Sun, to be re-accumulated back onto Mercury. A hit and run collision [2] provides a cleaner solution, and in most cases, much lower levels of shock and potentially greater retention of volatiles. However, hit and run is usually followed by subsequent re-collision, and ultimate accretion; an embryo's survival after being a hit and run projectile is unlikely in any single instance. Most of the original planetary embryos have been accreted by Earth and Venus; unaccreted planets are lucky. Here we show that the surviving terrestrial planet population is likely to have about as many hit and run survivors, as it is to have untouched survivors. That is, the differences between Mercury and Mars can be explained in a statistical manner as a consequence of accretionary attrition. We consider applications to asteroids, meteorites and exoplanets.

1. Mercury and Mars

Earth, Venus, Mars and some of the largest asteroids have massive silicate mantles surrounding iron cores, and chondritic compositions. Against this backdrop are anomalies like the iron planet Mercury, and the Moon with almost no core, and metallic asteroids like Psyche. The Moon can be explained by giant impact, but for Mercury a giant impact [1] is problematic. Mercury must retain substantial volatiles after its obliteration [e.g. 3] and must somehow avoid accreting its ejected silicates [4].

Impact hydrocode simulations using smooth particle hydrodynamics (SPH) have shown [2] that a proto-Mercury about 3 times its present mass can be stripped of its mantle in one energetic hit and run collision [5] with a larger planet, proto-Venus or proto-Earth. To preserve volatiles we also consider the scenario of multiple hit-and-runs in succession, with each event occurring at relatively low impact velocity (~10 km/s) in a glancing blow. If this sounds like an exotic recipe for making an iron planet, it is. But the point is that the non-exotic recipe is the one that makes Earth and Venus – that is, the one that gathers everything up. The stuff that is left behind, is what concerns us when considering Mercury and Mars, planets an order of magnitude less massive than the others. They are all exotic, and we apply a simple statistical argument to address this concept.

We show that small relics (Mercury, Psyche) can be survivors of repeated hit and run collisions, as witnessed in recent dynamical trials [6]. Specifically, the statistics of attrition makes one mantle-stripped planet (Mercury) probable, alongside one relatively undisrupted planet (Mars), if ~20 comparable progenitors were accreted by Venus and Earth. This is illustrated in Figure 1.

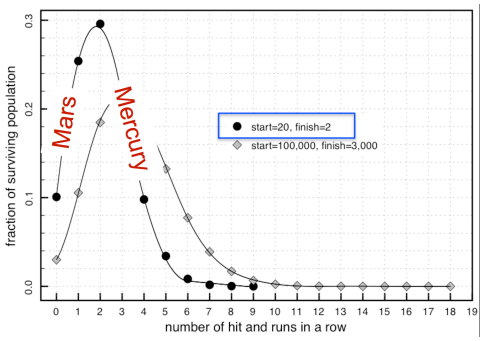

Figure 1. Starting from 20 initial embryos, the likelihood of having suffered *h* hit and run collisions in a row increases with the degree of attrition. So for the case of 20 embryos accreting until there are 2 unaccreted original bodies, about half the time you get a Mars-like planet (one or zero hit and runs), and about half the time you get a Mercury-like planet (several hit and runs).

2. Vesta and Psyche

For iron asteroids the 'missing mantle paradox' also looms prominent. And how do we strip away so much mantle rock, in some cases [7, 8] down to a bare iron core, while leaving asteroids like Vesta presumably intact? [9] The problem here is quite analogous to Mercury, whose target (proto-Venus or proto-Earth) is the hiding ground for its lost mantle. According to the hit and run hypothesis, the sink for all this missing silicate is the larger accreted bodies at the top of the feeding chain.

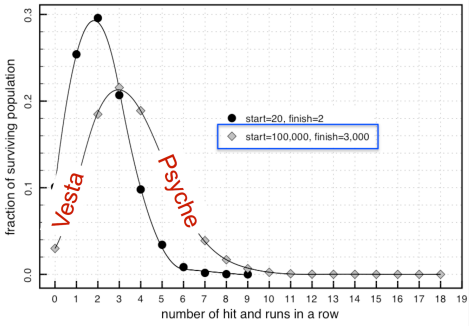

Figure 2. Same as Figure 1, but for 100,000 planetesimals accreting onto larger bodies, until 3,000 are left. In this case attrition is stronger, and the survivors are more exotic. About half the unaccreted population has 0-3 hit and runs, and the half of the population has 3-7 hit and runs. In reality collisional accretion and non-accretion is a very messy thing, and the *h*-number simply represents the characteristic number of non-accretionary collisions suffered by the unaccreted remnant bodies.

3. Discussion

The missing mantle paradox is only relevant to those few pairwise encounters that do not accrete both bodies. It is not a paradox, because the mantle is in plain view, accreted onto larger planets. Small planets are lucky unaccreted survivors, and the resulting attrition bias is manifested as compositional diversity and a preponderance of iron relics.

References

[1] Benz, W., Slattery, W. L. & Cameron, A. G. W. Collisional stripping of Mercury's mantle. *Icarus* **74**, 516–528 (1988).

[2] Asphaug, E., & Reufer, A. Mercury and other iron-rich planetary bodies as relics of inefficient accretion. *Nature Geoscience*, **7**, 564–568 (2014)

[3] Peplowski, P. N. *et al.* Radioactive Elements on Mercury's Surface from MESSENGER: Implications for the Planet's Formation and Evolution. *Science* **333**, 1850–(2011).

[4] Gladman, B. & Coffey, J. Mercurian impact ejecta: Meteorites and mantle. *Meteoritics & Planetary Science* **44**, 285–291 (2009).

[5] Asphaug, E., C. B. Agnor, Q. Williams (2006). Hit-and-run planetary collisions, *Nature* **439**, 155-160

[6] Chambers, J. E. Late-stage planetary accretion including hit-and-run collisions and fragmen- tation. *Icarus* **224**, 43–56 (2013).

[7] Yang, J., Goldstein, J. I. & Scott, E. R. D. Iron meteorite evidence for early formation and catastrophic disruption of protoplanets. *Nature* **446**, 888–891 (2007).

[8] Moskovitz, N. A. & Walker, R. J. Size of the group IVA iron meteorite core: Constraints from the age and composition of Muonionalusta. *Earth Planet. Sci. Lett.* **308,** 410–416 (2011).

[9] Consolmagno, G. J., Golabek, G. J., Turrini, D., Jutzi, M., Sirono, S., Svetsov, V., & Tsiganis, K. (2015). Is Vesta an intact and pristine protoplanet?. *Icarus* **254**, 190-201.

EPSC Abstracts
Vol. 10, EPSC2015-826, 2015
European Planetary Science Congress 2015

Color variations on Victoria quadrangle: support for the geological mapping

F. Zambon (1), V. Galluzzi (2), C. Carli (1), L. Giacomini (3), M. Massironi (3, 4), P. Palumbo (1, 2), L. Guzzetta (5), P. Mancinelli (6), V. Vivaldi (3, 4), L. Ferranti (5, 7), C. Pauselli (6), A. Frigeri (1), M. Zusi (1), R. Pozzobon (4), G. Cremonese (4), S. Ferrari (8), F. Capaccioni (1); francesca.zambon@iaps.inaf.it

(1) Istituto di Astrofisica e Planetologia Spaziali, Istituto Nazionale de Astrofisica, Rome, Italy, (2) Dipartimento di Scienze e Tecnologie, Università degli Studi di Napoli "Parthenope", Naples, Italy (3) Dipartimento di Geoscienze, Padova University, Padova, Italy (4) INAF, Osservatorio Astronomico di Padova, Padova, Italy (5) INAF, Osservatorio Astronomico di Capodimonte, Naples, Italy (6) Dipartimento di Fisica e Geologia, Università degli studi di Perugia, Perugia, Italy (7) DiSTAR, Università degli Studi di Napoli "Federico II", Naples, Italy (8) German Aerospace Center, DLR, Rutherfordstrasse 2, 12489 Berlin, Germany

Introduction

Mercury is the closest planet to the Sun. Its extreme thermal environment makes it difficult to explore onsite. In 1974, Mariner 10, the first mission dedicated to Mercury, covered 45% of the surface during of the three Hermean flybys [1]. For about 30 years after Mariner 10, no other mission has flown to Mercury. Many unresolved issues need an answer, and in recent years the interest about Mercury has increased. MESSENGER mission contributed to understand Mercury's origin, its surface structure, and the nature of its magnetic field, exosphere, and magnetosphere [1]. The Mercury Dual Imaging System (MDIS) provided a global coverage of Mercury surface with variable spatial resolution. MDIS is equipped with a narrow angle camera (NAC), dedicated to the study of the geology and a wide angle camera (WAC) with 12 filters useful to investigate the surface composition [2]. Mercury has been divided into 15 quadrangles for mapping purposes [3]. The mapping process permits integration of different geological surface information to better understand the planet crust formation and evolution. Merging spectroscopically data is a poorly followed approach in planetary mapping, but it gives additional information about lithological composition, contributing to the construction of a more complete geological map [e.g. 4]. Recently, [5] proposed a first detailed map of all the Victoria quadrangle (H2). Victoria quadrangle is located in a longitude range between 270°E and 360°E and a latitude range of 22.5°N and 65°N, and it was only partially mapped by Mariner 10 data [3].
Here we investigate the lithological variation by using the MDIS-WAC data to produce a set of color map products which could be a support to the geological mapping [5]. The future ESA-JAXA mission to Mercury, BepiColombo, will soon contribute to improve the knowledge of Mercury surface composition and geology thanks to the Spectrometer and Imagers for MPO BepiColombo-Integrated Observatory SYStem (SIMBIO-SYS) [6].

Dataset analysis

To derive the color filter mosaics, we selected the MDIS-WAC data from the PDS-ATLAS database (http://pds-imaging.jpl.nasa.gov /Atlas/). MESSENGER mission had onboard also a punctual hyperspectral spectrometer, MASCS-VIRS [7], but considering that Mercury reflectance spectra does not show absorption features and the MASCS coverage is not global, at least for this first step we do not considered the MASCS spectra for our purposes. We chose images with incidence, emission and phase angles between 0° and 70°, to have a better coverage of the quadrangle. We chose 8 of the 12 filters available according to literature [8, 9] (See Table 1). The data have been photometrically corrected with Hapke method [10], using the parameters derived by [11]. For each filter in this preliminary stage, we create a global mosaic at 200 mpp and co-registered it to the others. Finally we generate a file of the whole quadrangle containing the filter mosaics in order of wavelength.

Victoria quadrangle

The Victoria quadrangle is characterized mainly by intercrater plains material, but it also encompasses

patches of intermediate plains within its central area and smooth plains to the north. The quadrangle is named after its most prominent structure Victoria Rupes (lon ~328°E, lat 35°N-55°N), which is a single east-facing lobate scarp, suggesting east–west compression with the hanging wall transported eastward [5, 12, 13]. In this quadrangle both pyroclastic deposits [14, 15] and hollows [16, 17] have also been recognized. Analyzing the 8 filters cube of all the quadrangle we can highlight the principal and minor spectral units (e.g. [8, 9]).

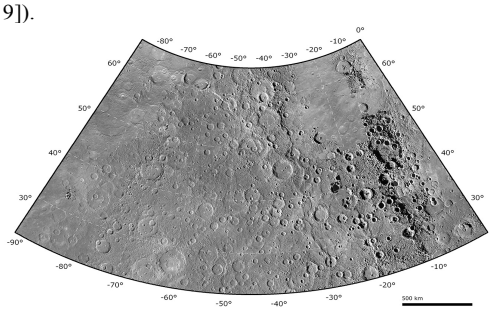

Fig. 1: MESSENGER MDIS 250 mpp mosaic of the Victoria quadrangle. *Credits: NASA/Johns Hopkins University Applied Physics Laboratory/Carnegie Institution of Washington*

Filters	Wavelength (nm)
F	430
C	480
E	560
D	630
G	750
L	830
J	900
K	1000

Table 1: Filters selected to produce the MDIS-WAC mosaics.

Implications

The color filter mosaic of the quadrangle with a resolution of 200mpp, will allow to correlate the recognized units to the color variation, indicative of different surface lithologies, this will provide a critical analysis of the results derived from classical planetary photo-interpretation. A discussion of the differences between the spectral recognition of those lithologies and the morphologic and tectonic evidences will also improve the interpretation of the surface. Combining different methods for geological interpretation of Mercury's surface is crucial in order to improve planetary geologic mapping results and thus to better understand the origin and evolution of the planet. Moreover this approach could be essential to better define specific targets for the SIMBIO-SYS team.

Acknowledgements

This activity has been realized under the BepiColombo Agenzia Spaziale Italiana (ASI) contract to the Istituto Nazionale di Astrofisica (INAF) no I/022/10/0.

References

[1] Solomon, S. C, et al., MESSENGER Mission Overview, 2007, Space Sci. Rev. [2] Hawkins, S. E. et al. The Mercury Dual Imaging System on the MESSENGER Spacecraft, 2007, Space Sci. Rev. [3] Davies, M., et al., Altas of Mercury, 1978, NASA SP-423. [4] Giacomini, L. et al., Spectral analysis and geological mapping of the Daedalia Planum lava field (Mars) using OMEGA data, 2012, Icarus. [5] Galluzzi, V., 2015, PhD thesis. [6] Flamini, E. et al., SIMBIO-SYS: The spectrometer and imagers integrated observatory system for the BepiColombo planetary orbiter, 2010, PSS. [7] Espiritu, R. and Malaret, E., Experiment Data Record Software Interface Specification for the MESSENGER Mercury Atmospheric and Surface Composition Spectrometer/ Visible and Infrared Spectrograph (MASCS/VIRS) SIE-06-045 D, 2012, MASCS/VIRS EDR SIS Version 2.2. [8] Denevi, B., et al., The Evolution of Mercury's Crust: A Global Perspective from MESSENGER, 2009, Science. [9] Blewett, D., et al., Multispectral images of Mercury from the first MESSENGER flyby: Analysis of global and regional color trends, 2009, Earth and Planetary Science Letters. [10] Hapke, B., et al., Theory of Reflectance and Emittance Spectroscopy, 2012, 2nd edition, Cambridge University Press. [11] Hapke, B., et al., Theory of Reflectance and Emittance Spectroscopy, 2012, 2nd edition, Cambridge University Press. [12] Rothery, D. A., et al., Planet Mercury, 2015, Springer. [13] Byrne, P., et al., Mercury's global contraction much greater than earlier estimates, 2014, Nature Geoscience. [14] Kerber et al., Explosive volcanic eruptions on Mercury: Eruption conditions, magma volatile content, and implications for interior volatile abundances, 2009, Earth and Planetary Science Letters. [15] Goudge, T. et al., 2014, Global inventory and characterization of pyroclastic deposits on Mercury: New insights into pyroclastic activity from MESSENGER orbital data, JGR. [16] Blewett, D., et al., Hollows on Mercury: MESSENGER Evidence for Geologically Recent Volatile-Related Activity, 2011, Science. [17] Blewett, D. et al., Mercury's hollows: Constraints on formation and composition from analysis of geological setting and spectral reflectance 2013, JGR.

EPSC Abstracts
Vol. 10, EPSC2015-927, 2015
European Planetary Science Congress 2015

Timing of activity of two fault systems on Mercury

V. Galluzzi (1,2), L. Guzzetta (3), L. Giacomini (4), L. Ferranti (5), M. Massironi (4) and P. Palumbo (1,2)
(1) Dipartimento di Scienze e Tecnologie, Università degli Studi di Napoli "Parthenope", Naples, Italy, (2) INAF, Istituto di Astrofisica e Planetologia Spaziali, Rome, Italy, (3) INAF, Osservatorio Astronomico di Capodimonte, Naples, Italy, (4) Dipartimento di Geoscienze, Università degli Studi di Padova, Padova, Italy, (5) DiSTAR, Università degli Studi di Napoli "Federico II" (valentina.galluzzi@iaps.inaf.it).

Abstract

Here we discuss about two fault systems found in the Victoria and Shakespeare quadrangles of Mercury. The two fault sets intersect each other and show probable evidence for two stages of deformation. The most prominent system is N-S oriented and encompasses several tens to hundreds of kilometers-long and easily recognizable fault segments. The other system strikes NE-SW and encompasses mostly degraded and short fault segments. The structural framework of the studied area and the morphological appearance of the faults suggest that the second system is older than the first one. We intend to apply the buffered crater counting technique on both systems to make a quantitative study of their timing of activity that could confirm the already clear morphological evidence.

1. Introduction

NASA MESSENGER mission confirmed the predominantly contractional deformation of Mercury's surface [1], [2]. The latest global structural mapping of Mercury revealed almost 6000 contractional structures [3]. The surface expression of most of these structures is represented by lobate scarps, which are steep scarps characterized by "a gently sloping back limb" [3] and are asymmetrical in cross-section [2]. They were described for the first time by [4] and interpreted as surface breaking thrusts. Usually, Mercury's thrusts are thought to be the expression of global contraction due to core solidification [4] or to a combination of global contraction, tidal despinning [5] and probably, mantle convection [6]. While several simulations take into consideration all of the three tectonic models, e.g. [7], [8], the timing and the actual development of these events is not yet clear. These faults often cut Calorian units, therefore their activity continued after the emplacement of these young terrains, e.g. [9]. A recent study of Hermean structures revealed the possibility that two stages of deformation might have occurred on a portion of the planet [10]. Thus, an accurate study of the interaction between the various Hermean fault systems is crucial to understand the timing of tectonic events. Our study aims at understanding the structural framework and timing of activity of two fault systems encompassed between the Victoria and Shakespeare quadrangles of Mercury.

2. Structural framework

The geological map of the Victoria quadrangle that was completed recently [11] revealed some new NE-SW oriented scarps, which are less prominent than lobate scarps and have a more degraded morphology that is often visible just from slight topographical changes. These structures continue to the west in the nearby Shakespeare quadrangle and they all seem to belong to the same system. On the other hand, the prominent Victoria Rupes, Endeavour Rupes and Antoniadi Dorsum lobate scarps (morphological *dorsa* are sometimes addressed to as high-relief ridges) form a N-S system that cuts the NE-SW system, which is interrupted in correspondence of a N-S fault-free topographic bulge [11], whose eastern margin was also interpreted as a fold-and-thrust belt by [3].

3. Timing analysis

The timing analysis of the two fault systems activity is done by means of morphological evidences, cross-cutting relationships and crater counting analysis. While the first two methods imply a qualitative description, the last method can provide quantitative evidence for different deformation stages.

3.1 Buffered crater counting

The "buffered crater counting" technique by [12], [13] has been hitherto used by [14] and [15] to assess fault

ages. It consists in counting craters unfaulted/undeformed by the nearby faults (in this work we consider fault buffer distance ≤ 1.5D, where D is the diameter of the crater), to get a cumulative size-frequency distribution (CSFD) that can be either compared to other CSFDs to get relative ages, or to production functions to get fault absolute ages. Buffered crater counting performed on the N-S system (Figure 1) already provided a relative age result that is younger than the smooth plains unit. Gathering data also from the NE-SW system will permit to compare the relative age of the two systems and verify the morphological evidence.

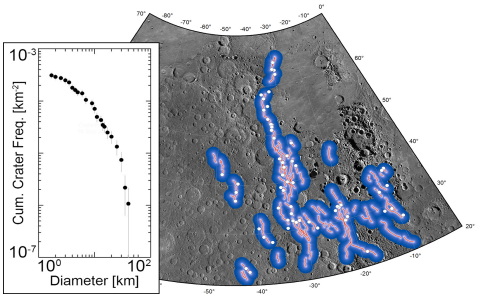

Figure 1. Example of a buffered crater count performed on the N-S fault system of the Victoria quadrangle (based on 61 counted craters). Basemap: MESSENGER MDIS 250 mpp mosaic (NASA/JHUAPL/CIW).

4. Summary and Conclusions

By analyzing the structural framework of the area between the Victoria and the Shakespeare quadrangles, two fault systems showing interesting cross-cutting relationship were found. The morphological evidence and the fault segments distribution seem to suggest that the NE-SW system is older than the N-S system [11]. This also seems to suggest that two stages of deformation acted on this area as also argued by [10] on another location of Mercury. The buffered crater counting method applied on both systems will permit to better estimate their relative age, thus getting us closer to understanding the evolution of Mercury.

Acknowledgements

This research was supported by the Italian Space Agency (ASI) within the SIMBIOSYS project (ASI-INAF agreement no. I/022/10/0).

References

[1] Watters, T.R. Solomon, S.C., Robinson, M.S. et al.: The tectonics of Mercury: The view after MESSENGER's first flyby, Earth and Planetary Science Letters, Vol. 285, pp. 283–296, 2009.

[2] Byrne, P.K., Klimczak, C., Şengör, A.C. et al.: Mercury's global contraction much greater than earlier estimates, Nature Geoscience, Vol. 7, pp. 301–307, 2014.

[3] Watters, T.R. & Nimmo, F.: The tectonics of Mercury, in Watters, T. R. & Schultz, R. A. (eds), Planetary tectonics, Cambridge University Press, 2010.

[4] Strom, R.G., Trask, N.J. and Guest, J.E.: Tectonism and volcanism on Mercury. Journal of Geophysical Research, Vol. 80, pp. 2478–2507, 1975.

[5] Melosh, H.J. & Dzurisin, D.: Mercurian global tectonics: A consequence of tidal despinning?, Icarus, Vol. 35, pp. 227–236, 1978.

[6] King, J.S.: Pattern of lobate scarps on Mercury's surface reproduced by a model of mantle convection, Nature Geoscience, Vol. 1, pp. 229–232, 2008.

[7] Matsuyama, I. & Nimmo, F.: Gravity and tectonic patterns of Mercury: Effect of tidal deformation, spin‐orbit resonance, nonzero eccentricity, despinning, and reorientation, Journal of Geophysical Research: Planets (1991‐2012), Vol. 114, 2010.

[8] Klimczak, C., Byrne, P.K. and Solomon, S.C.: A rock-mechanical assessment of Mercury's global tectonic fabric, Earth and Planetary Science Letters, Vol. 416, pp. 82–90, 2015.

[9] Watters, T.R., Robinson, M.S., Bina, C.R. et al.: Thrust faults and the global contraction of Mercury, Geophysical Research Letters, 31, L04701, 2004.

[10] López, V., Ruiz, J. and Vázquez, A.: Evidence for two stages of compressive deformation in a buried basin of Mercury, Icarus, Vol. 254, pp. 18–23, 2015.

[11] Galluzzi V.: Structural analysis of the Victoria quadrangle (H2) of Mercury based on NASA MESSENGER data, PhD thesis, 2015.

[12] Tanaka, K.L.: A new time-saving crater-count technique, with application to narrow features, in: Reports of Planetary Geology Program, NASA TM-85127, 1982.

[13] Fassett, C.I. & Head III, J.W.: Valley network-fed, open-basin lakes on Mars: Distribution and implications for Noachian surface and subsurface hydrology, Icarus, Vol. 198, pp. 37–56, 2008.

[14] Giacomini, L., Massironi, M., Marchi, S. et al.: Age dating of an extensive thrust system on Mercury: implications for the planet's thermal evolution, Geological Society, London, Special Publications, Vol. 401, pp. 291–311, 2015.

[15] Kneissel, T., Michael, G.G., Platz, T. et al.: Age determination of linear surface features using the Buffered Crater Counting approach – Case studies of the Sirenum and Fortuna Fossae graben systems on Mars, Icarus, Vol 250, pp. 284–394, 2015.